A. Jurjiu, R. Dockhorn, O. Mironova, J.-U. Sommer

Two universality classes for random hyperbranched polymers

Erstveröffentlichung in / First published in:
Soft Matter. 2014, 10(27), S. 4935–4946 [Zugriff am: 04.11.2019]. Royal Society of Chemistry. ISSN 1744-6848.

DOI: https://doi.org/10.1039/c4sm00711e

Soft Matter

PAPER

View Article Online
View Journal | View Issue

Cite this: *Soft Matter*, 2014, **10**, 4935

Two universality classes for random hyperbranched polymers

A. Jurjiu,*[a] R. Dockhorn,[a] O. Mironova[a] and J.-U. Sommer[ab]

Received 1st April 2014
Accepted 4th April 2014

DOI: 10.1039/c4sm00711e

www.rsc.org/softmatter

We grow AB_2 random hyperbranched polymer structures in different ways and using different simulation methods. In particular we use a method of *ad hoc* construction of the connectivity matrix and the bond fluctuation model on a 3D lattice. We show that hyperbranched polymers split into two universality classes depending on the growth process. For a "slow growth" (SG) process where monomers are added sequentially to an existing molecule which strictly avoids cluster–cluster aggregation the resulting structures share all characteristic features with regular dendrimers. For a "quick growth" (QG) process which allows for cluster–cluster aggregation we obtain structures which can be identified as random fractals. Without excluded volume interactions the SG model displays a logarithmic growth of the radius of gyration with respect to the degree of polymerization while the QG model displays a power law behavior with an exponent of 1/4. By analyzing the spectral properties of the connectivity matrix we confirm the behavior of dendritic structures for the SG model and the corresponding fractal properties in the QG case. A mean field model is developed which explains the extension of the hyperbranched polymers in an athermal solvent for both cases. While the radius of gyration of the QG model shows a power-law behavior with the exponent value close to 4/5, the corresponding result for the SG model is a mixed logarithmic–power-law behavior. These different behaviors are confirmed by simulations using the bond fluctuation model. Our studies indicate that random sequential growth according to our SG model can be an alternative to the synthesis of perfect dendrimers.

I. Introduction

A fundamental and long-standing problem in polymer physics is to deduce the relationship between the topology of a macromolecule and its static and dynamic properties. Paradigmatic for the broad interest are regular dendrimers[1–14] but also general treelike structures, so-called hyperbranched polymers.[3,8,9,11,15–32] Because of their architectural similarities, hyperbranched polymers have attracted considerable attention as possible cheaper alternatives to the more precise dendrimers. From the chemical side dendrimers are not that simple to prepare. Their geometrical perfection requires either inside-out or outside-in procedures consisting of several reaction steps, between which one has to purify the samples from the unwanted reaction by-products.[33,34] Hyperbranched polymers are commonly synthesized in batch reactions and are, in principle, not limited in their growth compared to dendrimers where the chemical synthesis usually stops after five or six generations due to the exponential increase of the number of branches at each generation.

Also for dendrimers with flexible spacers their static and dynamical properties are controlled by random conformations and thus by statistical properties. It is an open question whether hyperbranched polymers which in addition have random structural properties can be an alternative for diverse applications. One hurdle here is the fact that hyperbranched polymers can be obtained from different reaction pathways which makes it even more difficult to predict and to control their actual properties in a statistical ensemble.

Previous studies,[35–43] based on mean-field models, indicated that random hyperbranched polymers have a self-similar (fractal) architecture and their spectral dimension has been calculated to be $d_s = 4/3$. In ref. 35–39 it has been shown that the radius of gyration of random hyperbranched polymers scales with the total number of monomers, N, according to

$$R_0 \sim N^{\nu} \sim N^{1/4}, \quad (1)$$

with ν related to the fractal dimension according to $\nu = 1/d_f$ thus leading to $d_f = 4$. Recently, Konkolewicz *et al.*[44,45] have derived a rate-theory based model for the growth of randomly hyperbranched polymers consisting of monomers of the form ABC. The growth of the structures was realized by sequentially adding new units, a method which avoids cluster–cluster aggregation. In their case the polymerization involved both B–A and C–A links and it was assumed that the B groups were more reactive,

[a]*Leibniz Institut für Polymerforschung Dresden e.V., Hohe Strasse 6, D-01069, Dresden, Germany. E-mail: Jurjiu@ipfdd.de*

[b]*Technische Universität Dresden, Institut für Theoretische Physik, Zellescher Weg 17, D-01069, Dresden, Germany*

resulting in the C groups being potential branching points. Despite the previous studies which associated the hyperbranched polymers with fractals, they reported a logarithmic behavior for the radius of gyration as a function of N for their type of randomly hyperbranched structures instead of a power law as expected for fractals. We note that all these results are obtained by ignoring excluded volume interactions between monomers.

In this work we focus on the topology and static properties of the random hyperbranched polymers of type AB_2. The A and B represent functional groups that can react with each other but not with themselves. We show that the AB_2 random hyperbranched polymers split into two universality classes. Depending on the synthetic pathway either a fractal or a dendrimer-like topology is obtained. In particular we consider two cases: first, a sequential growth by adding monomers and strictly avoiding cluster–cluster aggregation. Second, a growth process where the cluster–cluster aggregation is allowed. Since the cluster aggregation or step reaction is a very fast process which can occur at high monomer densities we call this pathway the "quick growth" (QG) model while we call the sequential process which in reality requires very controlled conditions the "slow growth" (SG) model in the following. A sketch of the two types of growth is shown in Fig. 1. Here, the slow growth model is illustrated on the left hand side of the figure and the quick growth model on the right hand side. Both models yield random hyperbranched polymers with functionality $f = 3$ per monomer unit. In Appendices A and B we provide a detailed description of both growth processes and how they are implemented in our simulations. We note that already Hölter and Frey[46] have proposed a synthetic pathway for slow addition of AB_2 and these authors have reported a considerable increase of the degree of branching using this route.

We use two methods to create and investigate hyperbranched polymers: the model of Generalized Gaussian Structures (GGS)[5,11,15,47–51] applied to the connectivity matrix, and computer simulations using the Bond Fluctuation Model (BFM).[52,53] The latter allows us to switch on or off the excluded volume interactions. The GGS model is the natural extension of the Gaussian chain model to more complex geometries and does not take into account excluded volume constraints. The advantage of using the GGS model is that it allows one to explore very efficiently the structural properties, as well as the static and dynamical properties of arbitrarily connected polymers by making use of the eigenvalues and eigenvectors of the connectivity matrix.

We develop a mean-field model for hyperbranched polymers which relates their radius of gyration in the presence of a good solvent to that without the excluded volume. The latter is given by the connectivity exclusively. We find a very good quantitative agreement between the mean-field model and our simulation results using the BFM for both universality classes. In particular, the radius of gyration for structures generated with the QG model shows a power-law behavior with an exponent close to 0.8, while the structures generated with the SG model show a mixed logarithmic and power-law behavior as the perfect dendrimers in a good solvent.[54]

The rest of this work is structured as follows: in the next section we introduce the theoretical models with which we perform our analysis. In Section III we present the results for the investigated quantities. Our conclusions are given in Section V. The details of the GGS analysis, spectral properties, and the creation of the hyperbranched polymers with the two methods are presented in Appendices A–C.

II. Theory

A. Hyperbranched polymers without excluded volume

The impact of monomer's connectivity on the physical properties of polymers can be rigorously calculated for "phantom" polymers by ignoring excluded volume interactions. By assuming harmonic entropic forces between the flexible repeat units static and dynamic properties can be calculated from a matrix structure describing the connectivity of the polymer. In the literature this model has obtained the more technical term "Generalized Gaussian Structures" or simply GGS.[5,11,15,47–51] Here

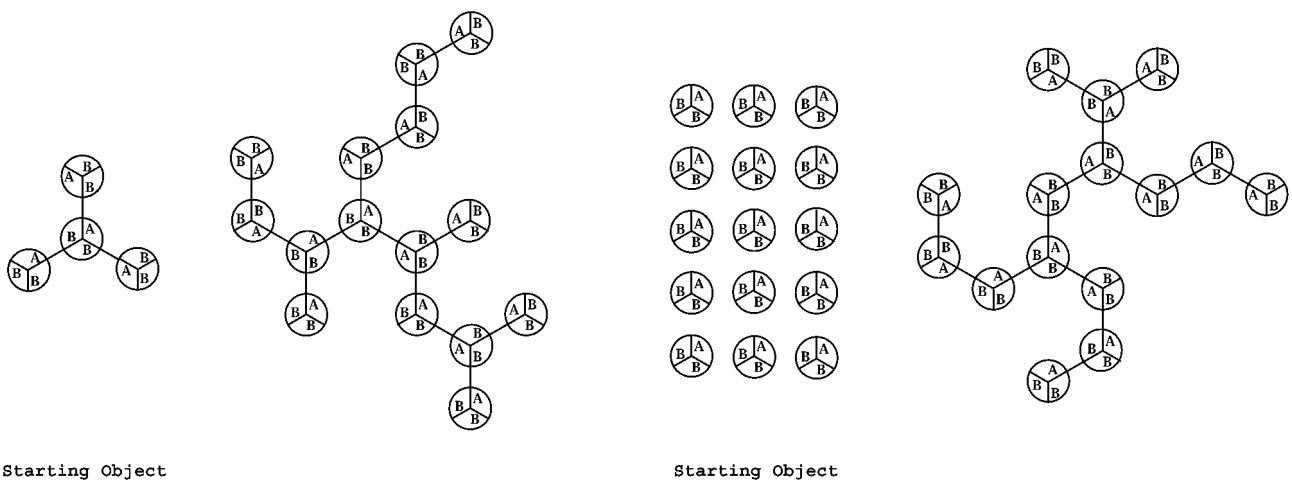

Fig. 1 SG model (left side) and QG model (right side).

we briefly summarize the main concept of this approach. The conformation of a polymer is given by the set of position vectors $\mathbf{R}_k$, where $\mathbf{R}_k(t) = (R_{xk}(t), R_{yk}(t), R_{zk}(t)) = (X_k(t), Y_k(t), Z_k(t))$ is the position of the k^{th} repeat unit at time t. As in the theory for flexible chains the repeat unit can be considered as a Kuhn segment.[55,56] For simplicity we will call this in the following a monomer. The GGS assumption is that the potential energy[49,51] is built only of harmonic terms, involving monomers directly bound to each other:

$$U(\{\mathbf{R}_K\}) = \frac{K}{2}\sum_{\beta,m,n} R_{\beta m} A_{mn} R_{\beta n} \tag{2}$$

In the sum all bonds are taken to be equal, with spring constant $K = 3k_BT/\langle l^2\rangle$ (where l is the bond length in thermal equilibrium); β runs over the components x, y and z. The connectivity is taken into account through the $N \times N$ matrix $\mathbf{A}$. By definition it is a real symmetric matrix whose nondiagonal elements A_{mn} equal -1 if the n^{th} and the m^{th} monomers are directly connected and 0 otherwise, while the diagonal elements A_{nn} equal the number of bonds originating from the n^{th} monomer. For a linear polymer $\mathbf{A}$ corresponds to the Rouse matrix used to describe the dynamics of ideal polymers.

A basic structural feature of a polymer is its radius of gyration. The mean squared radius of gyration is denoted by ${R_0}^2$ when the excluded volume constraints are not considered and by R^2 when they are taken into account. In the framework of the GGS model the mean squared radius of gyration depends only on the eigenvalue spectrum of the connectivity matrix[48,57,58]

$${R_0}^2 = \frac{\langle l^2\rangle}{N}\sum_{i=2}^{N}\frac{1}{\lambda_i}, \tag{3}$$

where λ_i are the eigenvalues of the connectivity matrix $\mathbf{A}$ and N is the total number of monomers. The eigenvalue $\lambda_1 = 0$ has to be excluded from the sum in eqn (3). The smallest non-zero eigenvalue λ_2 is connected with the extension and topology of the structure and the largest eigenvalue λ_N is determined by local branching properties. Further properties such as the average and the longest strand of the randomly connected structures can be calculated using also the eigenvectors of the connectivity matrix. Furthermore, the distribution of the eigenvalues can be related to self-similar properties of the polymers. Details are presented in Appendix A.

B. Excluded volume

Excluded volume interactions play a major role in highly branched polymers. In order to understand the effect of excluded volume on the size of branched polymers we will apply a Flory-type mean-field approach. The essential idea is to consider an elastic strand which extends from the center of the branched molecule to a terminal monomer.[64] We will assume that the swelling of the molecule due to excluded volume effects is balanced by the total elasticity of all independent strands. By further assuming that the distribution of the strands is represented by a characteristic length g, the free energy up to the third virial coefficient is given by

$$F = \frac{a}{2}\frac{N}{g}\left(\frac{R^2}{g}\right) + v_0\frac{N^2}{R^3} + w_0\frac{N^3}{R^6}, \tag{4}$$

where R denotes the characteristic extension of the molecule (radius of gyration) and a, v_0, and w_0 are numerical constants. Here, the length unit is given by the Kuhn segment and energies are given in units of k_BT. We note that this approach has been originally developed for perfect dendrimers[54,59] and is extended here to arbitrary branched structures. Without excluded volume interactions and under the given conditions the extension of the molecule is proportional to the extension of a single Gaussian strand, *i.e.*

$${R_0}^2 = b\cdot g, \tag{5}$$

where b denotes a constant which accounts for the numerical difference of the end-to-end distance of a single strand and the radius of gyration of the whole molecule. Using eqn (5), we can rewrite eqn (4) as follows

$$F = \frac{a'}{2}N\frac{R^2}{{R_0}^4} + v_0\frac{N^2}{R^3} + w_0\frac{N^3}{R^6}, \tag{6}$$

Taking this into account we obtain a minimum solution of eqn (6) of the general form $R(N, R_0)$.

Let us consider the case of a good solvent first, where we can ignore the third viral contribution. Then we obtain

$$R^2 = \kappa N^{2/5}{R_0}^{8/5}. \tag{7}$$

We note that there is only a single numerical constant, κ, which relates the observables. We note further that R_0 can be directly calculated in computer simulations by switching-off the excluded volume interactions for a given molecule. To illustrate the result we consider a few specific cases. For a linear chain, we have ${R_0}^2 = b_LN$ and hence we obtain Flory's classical result: ${R_L}^2 = \kappa_L N^{6/5}$. Next, we consider a perfect dendrimer. Here, the strand length is given by the product of spacer length, S, and the number of generations, G, *i.e.* $g = GS$. On the other hand we can write more generally for this case: ${R_0}^2 = S\cdot\ln(\alpha N/S)$, which reflects the exponential growth of a dendritic structure ($N/S \sim e^G$) and which defines the effective number of generations by $G = \ln(\alpha N/S)$. For this case we obtain ${R_{DD}}^2 = \kappa_{DD}N^{2/5}(GS)^{4/5}$. The latter result has been extensively tested in previous work for perfect dendrimers and is in very good agreement with computer simulations.[54] Finally, we consider a randomly branched polymer where the connectivity properties are controlled by a cluster–cluster aggregation mechanism as studied by Zimm and Stockmayer.[35] Here we have ${R_0}^2 = b_{ZS}N^{1/2}$ and thus we obtain ${R_{ZS}}^2 = \kappa_{ZS}N^{4/5}$.

Similarly, we can consider the case of θ – solvent, where we set $v_0 = 0$. This leads to

$$R^2 = \delta N^{1/2}R_0, \tag{8}$$

where δ is again a numerical constant. All results are summarized in Table 1. We note that for dendrimers and ZS-type hyperbranched polymers the θ – solvent does not

Table 1 Radius of gyration for three different polymer structures under various solvent conditions

R^2	Ideal	Good solvent	θ – solvent
Linear chain	N	$N^{6/5}$	$N \sim {R_0}^2$
Dendrimer	SG	$N^{2/5}R_0^{8/5}$	$N^{1/2}R_0$
ZS-type hyperbranched	$N^{1/2}$	$N^{4/5}$	$N^{3/4}$

correspond to the ideal or phantom case. The equivalence between the phantom molecule and theta-conditions is a specific result for linear chains. Even under poor solvent conditions, *i.e.* $R \sim N^{1/3}$, the dendrimers and ZS-type hyperbranched molecules are swollen with respect to the Gaussian case, a fact which is most dramatic for dendrimers, where under all solvent conditions a power-law behavior is obtained while the ideal conformation statistics leads to a logarithmic behavior.

We note that these considerations are made for neutral polymers only. In the case of partial or complete charging, depending on the parameters of the solution (degree of salt, temperature, pH), in particular, osmotically trapped counterions added to the free energy of eqn (6) lead to swelling of the structures. In previous work[60] we have shown that these effects lead to swelling of perfect dendrimers as compared to the neutral case. Since we did not consider charge effects on the present simulations we do not address this point any further.

III. Results

Hyperbranched structures are created by two methods: first, by *ad hoc* construction of the connectivity matrix. This corresponds to a random growth process without spatial restrictions. Second, we apply the bond fluctuation model (BFM)[52,53] to grow polymers respecting the excluded volume constraints in three dimensions during growth. In both cases we follow two pathways: in the quick growth (QG) model all monomers can react with each other and cluster–cluster aggregation is allowed. Only formation of cycles is prohibited. In the slow growth (SG) model starting from a core consisting of a few monomers hyperbranched polymers are obtained by sequentially adding single monomers. Here, cluster–cluster aggregation as well as formation of cycles are not possible. The details of the implementation of these algorithms can be found in Appendices B and C. Using the BFM we can furthermore switch-off the excluded volume constraints after growth in order to compare with the *ad hoc* generated structures. The eigenvalues of the connectivity matrices of the random hyperbranched structures are obtained through numerical diagonalizations.[61–63] All quantities to be presented are ensemble averaged. In the Gaussian approach (*ad hoc* construction of the connectivity matrix) we generate an ensemble of 1000 independent random structures of the same size and calculate the quantity for each generated structure. In the numerical simulations with BFM we averaged over at least 20 realizations.

A. Radius of gyration and excluded volume

The mean squared radius of gyration is a characteristic measure for the extension of the branched molecule. In Fig. 2 we show the results obtained by *ad hoc* construction of the connectivity matrix calculated using eqn (3) in the framework of the Gaussian model which does not account for excluded volume effects. In this model all bonds have the same length equal to one; thus the mean squared bond length $\langle l^2 \rangle = 1$. The solid line with triangles up represents the mean squared radius of gyration of the random hyperbranched structures built with the SG model and the solid line with triangles down represents the mean squared radius of gyration of the random hyperbranched structures built with the QG model. We used structures ranging from $N = 100$ to $N = 3000$.

In the double-logarithmic scales of the left hand side panel of Fig. 2 the mean squared radius of gyration of random hyperbranched structures created with the QG model appears as a straight line thus obeying a power law ${R_0}^2 \sim N^{\alpha}$. The best approximation to our data leads to $\alpha = 0.538$, the value being very close to the mean-field prediction of 1/2. Using eqn (A4) we find for the spectral dimension the value $d_s = 1.3$, very close to $d_s = 4/3$, the theoretical expected value of the spectral dimension of the random fractals.[35–43]

For the random hyperbranched structures obtained with the SG model the mean squared radius of gyration does not obey a power law and displays a concave curvature in the double logarithmic plot. To render this aspect clearer in the right hand side panel of Fig. 2 we present a semi-logarithmic plot, where the x-axis is logarithmic and the y-axis is linear. In this representation the mean squared radius of gyration of the random hyperbranched structures created with the SG model (the solid line with triangles up) appears as a straight line which clearly indicates a logarithmic behavior as that obtained for the dendrimers in the ideal case (phantom model).

In Fig. 3 we present the results for ${R_0}^2/\langle l^2 \rangle$ obtained from computer simulations by using BFM without excluded volume effects. For details see App. C and eqn (C1). The value of the mean squared bond length, $\langle l^2 \rangle$, was determined to be 7.389 for both types of random hyperbranched structures. We stress that excluded volume effects were switched off only in the relaxation process, while during the growth process of the structures the

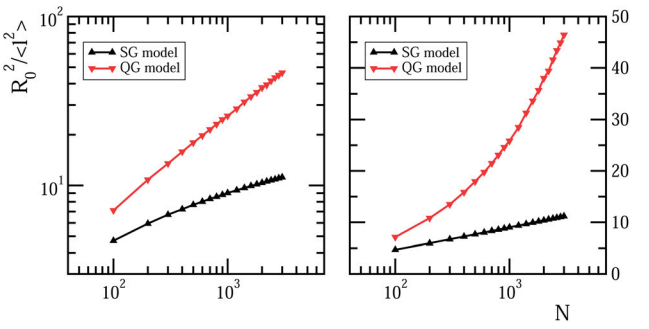

Fig. 2 The mean squared radius of gyration calculated in the framework of the Gaussian model using *ad hoc* construction of the connectivity matrix.

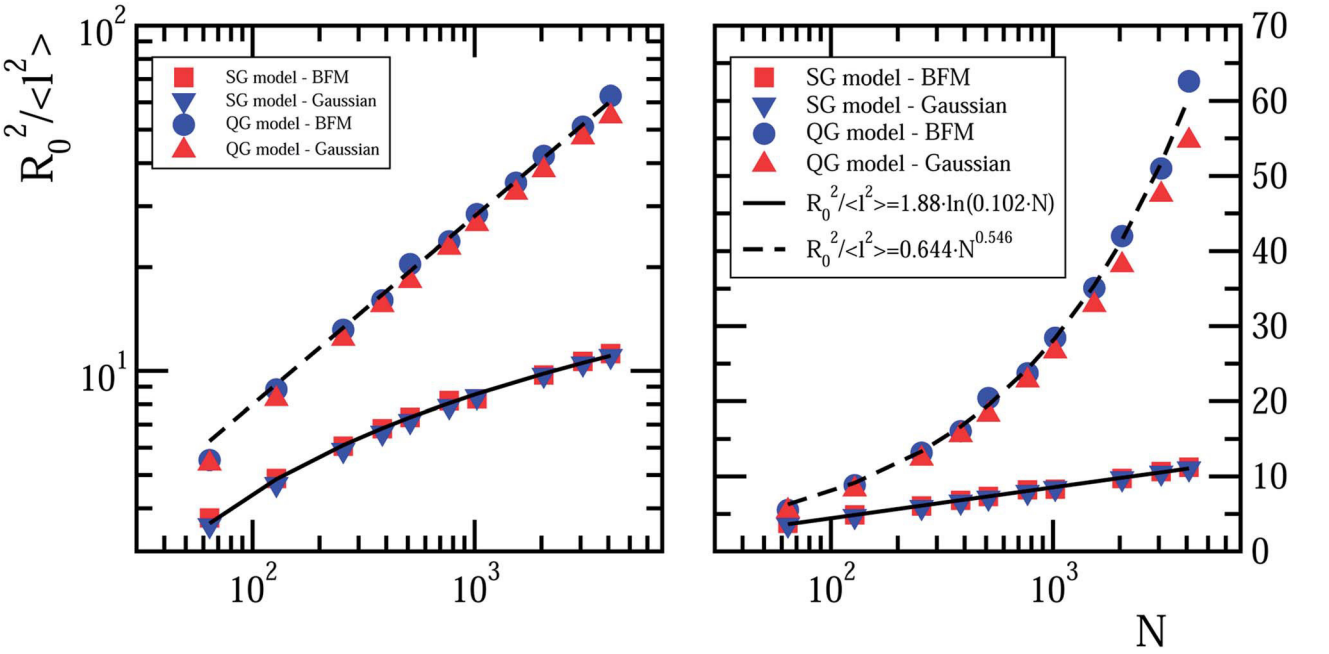

Fig. 3 The mean squared radius of gyration calculated using the BFM. The structures were grown under excluded volume constraints and then relaxed after switching-off excluded volume. For comparison R_0^2 calculated with the Gaussian model is also plotted.

excluded volume effects were always taken into account. The latter may lead to a different branching topology as compared to the *ad hoc* construction method. Therefore, we also plotted in Fig. 2 the results for R_0^2 calculated in the framework of the Gaussian model. In each panel of the figure, for both growing patterns (SG and QG) and evaluation models (BFM and Gaussian), we use structures extending from $N = 64$ to $N = 4096$. The squares represent the simulation data obtained for the structures built with the SG model and the circles represent the simulation data obtained for the structures created with the QG model. The results achieved in the framework of the Gaussian model are indicated with triangles down for the structures built with the SG model and with triangles up for the structures built with the QG model. Furthermore, we added the best fit (non-linear curve fitting with two parameters indicated in the figure with a solid line for SG and with a dashed line for QG) of the simulation results for the $R_0^2/\langle l^2\rangle$. For the QG model we used power law function, $R_0^2/\langle l^2\rangle = 0.644\ N^{0.546}$, and the value of the obtained exponent is again very close to the mean-field prediction of 1/2. For the simulation results of the $R_0^2/\langle l^2\rangle$ of the structures obtained with the SG model we used a logarithmic function, $R_0^2/\langle l^2\rangle = 1.88\ \ln(0.102\ N)$. As in Fig. 2, in the right hand side panel the corresponding semi-logarithmic view is displayed. The logarithmic behavior of the polymers created with the SG model is evident.

For all structures the equivalence between the BFM and the Gaussian model is evident. Even if in the simulations the structures were built in a realistic way taking into account the excluded volume constraints, the relaxation without excluded volume constraints leads to values for $R_0^2/\langle l^2\rangle$ very close to the ones achieved by using the properties of the connectivity matrix in the Gaussian model. This indicates that the topology of

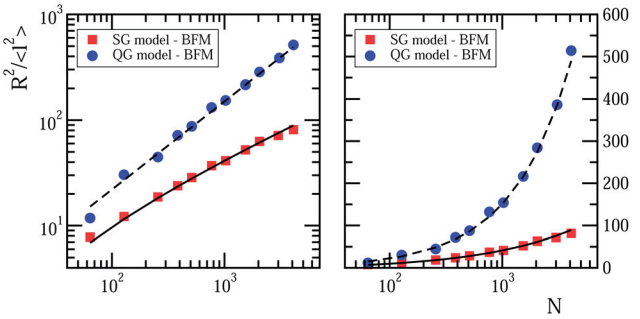

Fig. 4 The mean squared radius of gyration calculated using the BFM. The structures were grown and relaxed under excluded volume constraints. The solid and dashes lines display the behaviors as predicted by the mean field model in eqn (7) using the best fits (solid and dashed lines) of Fig. 3.

hyperbranched polymers in the range of polymerization considered here is not much influenced by the spatial restrictions during the growth process.

We now turn to the influence of good solvent conditions. These can be realized only in the BFM simulation. In Fig. 4 we display the behavior of the mean squared radius of gyration of both types of random hyperbranched structures under excluded volume effects. The squares represent the simulation results obtained for the structures generated with the SG model and the circles indicate the simulation results obtained for the structures generated with the QG model. The mean squared bond length in an athermal solvent is slightly extended and is given by $\langle l^2\rangle = 7.51$ for both types of random hyperbranched structures.

In order to rationalize the effects of a good solvent we apply the mean-field model according to eqn (7). This leaves us with

only one free parameter since the radius of gyration for the phantom case has been obtained before. For the structures built with the QG model, inserting into eqn (7) the expression of R_0^2 determined from the BFM simulations with excluded volume interactions switched off, one obtains $R^2 = \kappa N^{2/5}(0.644\, N^{0.546})^{4/5}$. Fitting the simulation results with its prediction we get $\kappa = 0.63$. We observe that the simulation results for $R^2/\langle l^2\rangle$ of the structure built with the QG model align well with the fitting curve (solid line), $R^2/\langle l^2\rangle = 0.443N^{0.837}$. Under excluded volume interactions the behavior of the $R^2/\langle l^2\rangle$ of the structures generated with QG is fully rendered by eqn (7) and its particularization, $R_{ZS}^2 = \kappa_{ZS}N^{4/5}$, to the structures built by the cluster–cluster aggregation mechanism.

In the same manner, for the structures generated with the SG model inserting into eqn (7) the expression R_0^2 obtained from the BFM simulations without excluded volume constraints one gets $R^2 = \kappa N^{2/5}(1.88\ln(0.102\ N))^{4/5}$. Fitting the results of the simulations with this expression yields $\kappa = 0.47$. The simulation results match very well the theoretical prediction (dashed line) which clearly indicates a mixed behavior, logarithmic–power-law and the polymers generated with the SG model are very well described by the mean-field approach.

Again, the similarities of the structures built with the SG model with perfect dendrimers are evident. The same behavior for the radius of gyration for perfect dendrimers with flexible spacers has been obtained recently in simulations.[54] This is also evident from the exponential growth of the dendrimers expressed as $R_0^2 = S\alpha\ \ln(\alpha N/S)$, which fully corresponds to the results for the SG model. In fact, we can associate structures of the SG model with an effective generation and spacer length of a perfect dendrimer as we will analyze further below in more detail.

On the right hand side of Fig. 4 we present again the semi-logarithmic view of $R^2/\langle l^2\rangle$ *vs.* N. For both types of random hyperbranched structures the fitting data lines from the left hand side panel holds very well also in the logarithmic-linear scales of the right hand side panel. This strengthens the fact that under excluded volume constraints the behavior of the mean squared radius of gyration of both types of random structures is described by eqn (7). We note that for the structures built with the SG model for very large values of N the power-law behavior will become dominant. However, within the range of polymerization studied in this work the asymptotic slope of 2/5 is not reached. An attempt to use a power-law fit for the largest SG-polymers is misleading since the logarithmic part is still essentially contributing up to $N = 6000$.

B. Mean strand lengths and spectral properties

We have seen above that the structures obtained by *ad hoc* construction of the connectivity matrix and by simulation in three dimensions are statistically equivalent within the range of parameters investigated here. This fact can be further substantiated by inspecting the connectivity matrix of the simulated structures (results not shown). In the following we will investigate some more properties of the connectivity structures and we can therefore restrict ourselves to the connectivity matrices obtained by the *ad hoc* construction method.

In Fig. 5 we display the averaged mean strand length, S_m; see Appendix A, in particular eqn (A9), for the random hyperbranched structures built with the SG model (solid line with triangles up) and for the random hyperbranched structures built with the QG model (dashed line with triangles down). In each panel, for both types of random hyperbranched polymers the number of monomers varies from $N = 100$ to $N = 3000$. Without excluded volume interactions and following the Gaussian statistics the extension of the molecule can be written according to eqn (5) as $R_0^2 \sim S_m$. Thus, one obtains $S_m \sim N^{\frac{2-d_s}{d_s}}$. For more details see Appendix A. In the double-logarithmic scales (left hand side of Fig. 5) the averaged mean strand length of random hyperbranched structures created with the QG model appears as a straight line which corresponds to a power law with an exponent of 0.504. Using this value in the above power law relation of S_m we determine the spectral dimension to be $d_s = 1.329$; this value should be compared with the theoretical value, $d_s = 4/3$, of the random fractals. The accuracy attained is certainly enough to assess that the random hyperbranched structures created with the QG model are random fractals.

The averaged mean strand length of the random structures built with the SG model does not display a power law behavior. This aspect is rendered more clearly in the semi-logarithmic

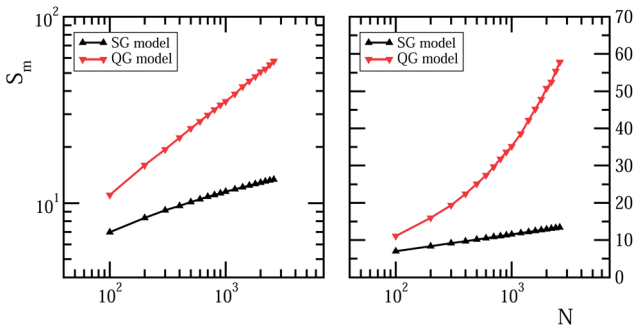

Fig. 5 The averaged mean strand length calculated in the framework of the Gaussian model using *ad hoc* construction of the connectivity matrix.

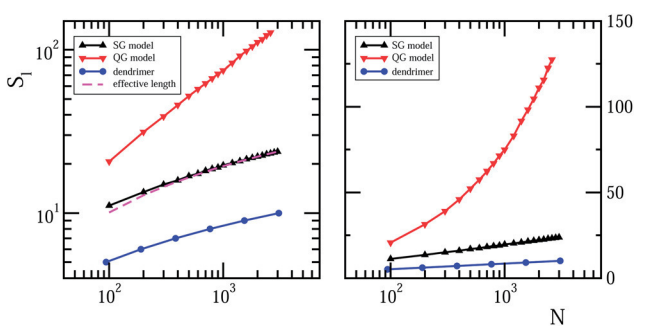

Fig. 6 The averaged longest strand length calculated in the framework of the Gaussian model using *ad hoc* construction of the connectivity matrix.

presentation (right hand side panel of Fig. 5). Here, the averaged mean strand length of the random hyperbranched structures built with the SG model appears as a straight line which indicates a logarithmic behavior in the ideal case.

In Fig. 6 we present the results for the averaged longest strand length, S_l, calculated based on eqn (A8), for the random hyperbranched structures created with the SG model (solid line with triangles up) and with the QG model (solid line with triangles down). In addition we added results for perfect dendrimers (solid line with circles) with functionality $f = 3$ and generations from $G = 5$ to $G = 10$. These values correspond to dendrimers whose number of beads varies from $N = 94$ ($G = 5$) to $N = 3070$ ($G = 10$). For the structures created with the QG model the averaged longest strand length appears as a straight line showing a power law behavior with the size. For dendrimers and for the structures created with the SG model a logarithmic behavior is found as clearly indicated in the right panel of Fig. 6.

When plotted in linear–linear scales the mean squared radius of gyration *versus* the averaged longest strand length (result not presented here) for random structures built with the QG model we found the slope of the curve to be nearly 1, showing that $R_0^2 \sim S_l$. This relationship indicates that the distribution of the strand lengths, $\rho(S)$, is non-singular and the average value is proportional to the largest value. Combining this relationship with eqn (A4) one finds the following power law behavior: $S_l \sim N^{\frac{2-d_s}{d_s}}$. From the plot we determined the slope of the averaged longest strand length of the structures created with the QG model to be equal to 0.542. Using the value of the slope in the above relationship for S_l we find the spectral dimension to be $d_s = 1.297$ again close to the theoretical value $d_s = 4/3$ of the random fractals.

Rescaling the asymptotic result obtained for the perfect dendrimer, $S_l = \alpha \ln(\beta N)$, with the expression $S_l = S\alpha \ln\left(\frac{\beta}{S}N\right)$ in order to fit the results of the SG structures we obtained $S = 2.8$. This indicates that the structures obtained with the SG model can be related to a perfect dendrimer with an effective spacer length of $S = 2.8$. The dashed line in the left panel indicates this fit. This result shows that the strand distribution is not singular and that the random structures built with the SG model are imperfect dendrimers.

In order to strengthen the classification of the random hyperbranched AB_2 polymers in two universality classes depending on the reaction process we finally consider the smallest eigenvalue, λ_{min}, of the connectivity matrix. In Fig. 7 we display the behavior of λ_{min} for the random structures created with the SG model (solid line with triangles up), for the random structures created with the QG model (solid line with triangles down), and for the perfect dendrimers (solid line with circles) with functionality $f = 3$. All three types of structures display straight lines in the double logarithmic representation, thus indicating power laws. Using linear fits we get the following values of the slopes: −1.505 for the QG model, −1.031 for the SG model, and −1.027 for the perfect dendrimers. As a guide to the eye the solid line indicates the slope −1. As outlined in Appendix A, this power law behavior can be again related to the spectral dimension. Using eqn (A2) with each value of the slope we determine the following values of the spectral dimension: for the structures built with the QG model, $d_s = 1.328 \simeq 4/3$; for the structures built with SG model, $d_s = 1.939 \simeq 2$; and for the perfect dendrimers, $d_s = 1.947 \simeq 2$, respectively. The first value again corresponds to the expected result for the random fractals, while the value of 2 corresponds to the Bethe lattice.

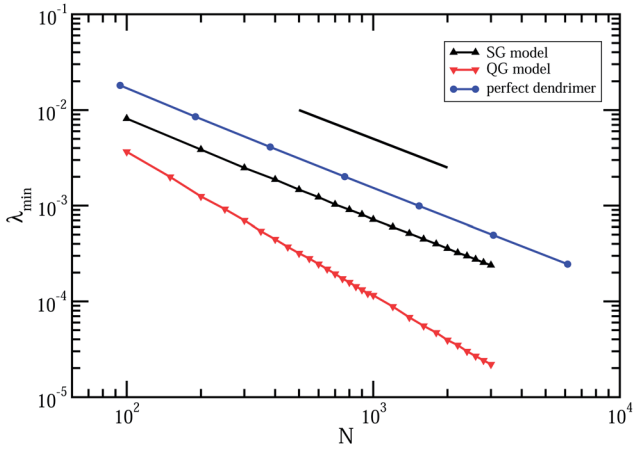

Fig. 7 The behavior of the smallest eigenvalue of the connectivity matrix. For guidance the simple solid line indicates the slope −1.

IV. Summary and conclusions

In this work we have shown that random hyperbranched polymers of type AB_2 can be subdivided into two universality classes depending on the reaction pathway. The structures obtained by adding reactive monomers sequentially (SG model) are imperfect dendrimers, while the structures obtained by step reaction allowing for cluster–cluster aggregation (QG model) are random fractals.

Hyperbranched polymers built from direct simulations using the Bond Fluctuation Model and from *ad hoc* construction of a random connectivity matrix have been compared. In the framework of the BFM the hyperbranched polymers are created under spatial constraints by respecting excluded volume interactions in 3D. The obtained polymers can nevertheless be relaxed both under excluded volume constraints and by switching off these constraints. The latter case allows for direct comparison with the *ad hoc* constructed connectivity matrices and also to obtain the reference values for the phantom radius of gyration as it is used in our mean-field approach.

For phantom polymers, the mean squared radius of gyration, R_0^2, of the structures created with the QG model shows a power-law behavior with the power law exponent value close to 0.5, which is the mean-field predicted value for random fractals under ideal conditions. Consequently, the value of the spectral dimension obtained from the power law exponent is very close to the theoretical value 4/3 of the spectral dimension of the random fractals. For the mean squared radius of gyration of the structures created with the SG model we found a logarithmic

behavior as for perfect dendrimers in the ideal conformation statistics. From this we claim that these structures are modified dendrimers.

The very good quantitative agreement of the results for $R_0^2/\langle l^2\rangle$ obtained in both simulation models for both universality classes shows that under the given range of degree of polymerization in our study, *i.e.* $N < 5000$, the spatial constraints in 3D during the growth process are not very important for the obtained random connectivity structure. We note that this conclusion can be further substantiated by considering the spectral properties of the polymers obtained with the BFM.

Using the extension of the different structures in the phantom case and assuming a non-singular distribution of strands originating from the center of the structure, we have proposed a Flory-type mean-field model to predict the extension of the hyperbranched polymers in a good solvent. We found that the measured mean squared radius of gyration of each type of random hyperbranched structure is entirely described by our mean-field model. Specifically, the particularization of the general eqn (7) to the structures built with the SG model, achieved by inserting their corresponding R_0^2 determined from the simulations with excluded volume interaction switched off, leads to an expression for R^2 that fully describes the results obtained from the simulations with excluded volume switched on for this type of random hyperbranched structures. In this case the dependence of the radius of gyration on the degree of polymerization is given by a mixed power-law and logarithmic behavior exactly as for perfect dendrimers in a good solvent. We have shown that SG hyperbranched polymers can be mapped to dendrimers with an effective spacer length.

For QG hyperbranched polymers the insertion of their R_0^2, determined from the simulations without excluded volume interactions, into the general eqn (7) leads to a form of R^2 that completely describes the results obtained from the simulations with excluded volume switched on for the ZS-type of random structures.

The analysis of the averaged mean strand length and the averaged longest strand length is in full accord with the results for the radius of gyration and proves for both universality classes the relationship $R_0^2 \sim S_m \sim S_l$.

The spectral dimension of the polymer connectivity can be directly read-off from the analysis of the smallest eigenvalue of the connectivity matrix. For the structures built with the QG model the value of their spectral dimension obtained from the power law exponent of the smallest eigenvalue is almost identical to the theoretical value of the spectral dimension of the random fractals which again proves that these structures are fractals. The spectral dimension of the structures created with the SG model determined from the corresponding power law exponent of the smallest eigenvalue corresponds to that of a perfect dendrimer which proves that the SG model leads to imperfect dendrimers.

Our study clearly demonstrates that the reaction pathway for hyperbranched polymers can change qualitatively the properties of the resulting structures. Sequentially adding reactive monomers to an existing cluster and by suppressing cluster–cluster aggregation lead to polymers which are identical to regular flexible dendrimers in major observable properties. Only the dominance of the cluster–cluster reactions leads to structures which correspond to random fractals.

A simple handwaving argument might be used to explain these findings: by adding reactive monomers sequentially every reactive site in the existing structure is chosen with an equal probability. Therefore, the reactive surface of the structure grows nearly isotropically. Since loops cannot be formed this leads to a dendritic structure. This is valid as long spatial constraints are not important which is equivalent to the claim that each reactive site is equally accessible. As we have seen in our direct simulations this is the case for up to several thousands of reactive units. Using this argument, we expect the same result if the conformation statistics leads to a rather rigid conformation as long as the accessibility of the reactive sites is not restricted. However, further simulations would be necessary to prove this. On the other hand, without breaking the isotropy of the reactive cluster–cluster aggregation leads to self-similarity in full analogy to the percolation transition on a Bethe-lattice.

Appendix

A Analysis of the GGS and the spectral properties

For large polymers we can define the density of eigenvalues $\rho(\lambda)$, *i.e.* the number of eigenvalues within a small interval $d\lambda$. Then eqn (3) of the main text can be rewritten as $R_0^2 = \langle l^2\rangle \int_{\lambda_{min}}^{\lambda_{max}} d\lambda\lambda\rho(\lambda)$. For isotropic and locally homogeneous fractal objects the density of eigenvalues, also called spectral density, shows a power-law behavior according to[64–66]

$$\rho(\lambda) \sim \lambda^{d_s/2-1} = \lambda^{(d_s-2)/2}, \tag{A1}$$

which defines the spectral dimension, d_s. For fractal objects with a spectral dimension less than 2 the smallest eigenvalue, λ_{min}, is inversely proportional to the time, t, needed by a random walker to explore the whole fractal of size N. Using the Zimm–Stockmayer relationship[35] $N \sim t^{d_s/2}$ one obtains

$$\lambda_{min} \sim t^{-1} \sim N^{-2/d_s}. \tag{A2}$$

Inserting eqn (A2) into eqn (3) of the main text, one gets for fractals with $d_s < 2$

$$R_0^2 \sim \lambda_{min}^{(d_s-2)/2}. \tag{A3}$$

Now, combining eqn (A2) and (A3) the mean squared radius of gyration reads

$$R_0^2 \sim N^{\frac{2-d_s}{d_s}}. \tag{A4}$$

The power law relationship of the mean squared radius of gyration from eqn (A4) is identical to that obtained by Cates.[67] For fractal objects with spectral dimension larger than 2 the mean squared radius of gyration does not depend on the

smallest eigenvalue, $\lambda_{\min}$, and thus it does not depend on the number of monomers, N. Such strongly connected phantom polymers would collapse and only excluded volume interactions can stabilize them.[48]

Within the concept of GGS also other topological properties can be calculated. First we consider the distance between two monomers i and j given by $R_{ij} = |\mathbf{R}_{ij}| = |\mathbf{R}_i - \mathbf{R}_j|$. The mean squared distances can be expressed in terms of eigenvalues λ_k and eigenvectors $\mathbf{Q}_k$ of the connectivity matrix **A**.[68,69]

$$\left\langle {R_{ij}}^2 \right\rangle = \langle l^2 \rangle \sum_{k=2}^{N} \left({\mathbf{Q}_k}^i - {\mathbf{Q}_k}^j \right)^2 {\lambda_k}^{-1}. \tag{A5}$$

We define the dimensionless distance measure (metrics) along the structure as

$$d_{ij} = \left(\frac{\left\langle {R_{ij}}^2 \right\rangle}{\langle l^2 \rangle} \right)^{0.5}. \tag{A6}$$

For structures without loops as considered here, d^2 gives the actual number of monomers separating the two monomers.

Using these metrics we can define the averaged mean strand length, S_m, and the averaged longest strand length, S_l, originating from the center of the structure and ending on terminal monomers. To determine the center of the random hyperbranched structure we use the following procedure: first we identify all terminal monomers which we denote by $\{n_t\}$. Non-terminal monomers are denoted by $\{n_{nt}\}$. For each non-terminal monomer, i, we calculate based on eqn (A5) and (A6) the distances from it to all terminal monomers and sum them, $D_i = \sum_{j \in \{n_t\}} d_{ij}$. Then, the center of the structure, c, is the monomer for which the sum of the distances to all terminal monomers is the smallest. It reads:

$$c = i, \quad \text{with} \quad D_i = \min_{i \in \{n_{nt}\}} (D_i) \tag{A7}$$

Having determined the center of the structure, we now calculate the distances from the center to all terminal monomers based on eqn (A5) and (A6). The longest strand length is given by:

$$S_l = d_{cj}, \quad \text{with} \quad d_{cj} = \max_{j \in \{n_t\}} \left(d_{cj} \right). \tag{A8}$$

The mean strand length is given by:

$$S_m = \frac{1}{N_t} \sum_{j \in \{n_t\}} d_{cj}. \tag{A9}$$

B Hyperbranched structures by *ad hoc* construction of connectivity matrix

In the slow growth model for the *ad hoc* construction of the connectivity matrix one starts from an object consisting of 4 monomers arranged in the starwise pattern, the central monomer being connected with three neighboring monomers. Each monomer has three links, two B links and one A link, and the allowed polymerization reaction occurs only between A and B links. A sketch of the model is shown in the left hand side of Fig. 1. In the starting object the central monomer has used all three links, the A link with a B from one neighbor and the two B links with the A links of the other two neighbors. Two neighboring monomers of the central monomer have each two B links free (those that put the A link with the B links of the central monomer) and the third neighboring monomer (the one that used a B link with the A of the central monomer) has an A and a B link free. To these six free links of the starting object one can add a new monomer. Generally, at every building step of the structure the reactive monomers, *i.e.* the ones that have at least one free link, are kept in a list. In this list a reactive monomer is counted twice if it has two free links or once if it has only one free link. The total number of reactive monomers in the list is equal to the total number of free links. In the second list we keep the number and the type of the links of each reactive monomer. As a simple example, for the starting object the list of reactive monomers consists of six monomer indices corresponding to the three neighboring monomers of the central monomer, each counted twice (because of having two free links each). The second list consists of numbers and types of the neighboring monomers of the central monomer; the first two neighbors have two free links of type B each, and the third neighbor has two free links, one of type A and one of type B.

From the starting object we grow the random hyperbranched polymer as follows: we randomly choose a monomer from the list of reactive monomers and from the second list for the chosen monomer we pick a link from its free links. Then for the candidate monomer (a new monomer that may be attached to the structure) we randomly choose a link from its three free links. If the chosen links, for the reactive monomer and for the candidate, are of the opposite types then the candidate monomer is added to the structure, and it is connected with a bond to the chosen reactive monomer. If the chosen links are of the same type then the attempt is rejected and we repeat the procedure. After a new monomer is added to the structure the two lists are updated and we iterate the procedure until the desired number of monomers in the structure is reached.

The authors in ref. 46 and 70 have defined the degree of branching (DB) of the general type of hyperbranched polymers AB_n. Specifically, for the degree of branching of the AB_2 hyperbranched polymers they have defined the following expression:

$$\mathrm{DB} = \frac{2D}{2D + L}, \tag{B1}$$

where D is the number of dendritic units (in our case the number of three-coordinated monomers) and L is the number of linear units (in our case the number of two-coordinated monomers). Without imposing additional constraints, the random hyperbranched polymers built with the slow growth model have the degree of branching, according to eqn (B1), DB = 0.66. We also generate with the SG model random polymers with DB smaller or larger than 0.66. For these structures we imposed an additional constraint in the building process; the addition of the new monomer should satisfy a predefined ratio

L/D. For example, in order to generate random structures with DB = 0.5 we imposed the additional constraint that each new monomer can be added to the structure if through its addition the ratio L/D will be equal to or slightly smaller then 2. For all quantities that we investigate in the framework of the Gaussian model we use only structures having DB = 0.66 with one exception in Fig. 3 where, in order to have the same degree of branching as the structures grown in computer simulations with BFM, we use structures with DB = 0.75.

It is important to note that the degree of branching does not change qualitatively the behaviors of the quantities on which we focus; the functional dependence of these quantities and the spectral properties do not change with the changing of the value of DB, if the mode of growth, *i.e.* avoiding cluster–cluster aggregations, is not changed. In fact the DB is an insufficient measure of the overall connectivity of the structure.

In the quick growth model one starts from a set of N free monomers, N being the desired number of monomers in the final structure. Each monomer from the starting set is a reactive monomer having two free links of type B and one free link of type A. A sketch of the QG model is displayed in the right hand side of Fig. 1. As in the case of the SG model we also use two lists. The first list contains the reactive monomers and each monomer is counted according to its number of free links. The list of the reactive monomers for the starting set consists of $3N$ elements (monomer number from 1 to N). In the second list we keep for each monomer the monomer number, its free links, and a cluster index used for preventing formation of loops. In the starting set for each monomer the monomer number and the cluster index are identical.

From the starting set of N free monomers we build the structure by trying to connect at each step two monomers with a bond. The procedure is as follows: from the list of reactive monomers one randomly chooses two monomers and from the second list for each chosen monomer one randomly picks a link from its free links. If the chosen links are of the same type the choice is rejected. In order to prevent loop formation within the same cluster we next check the cluster indices of the chosen monomers. If the chosen monomers have different cluster indices they are connected with a bond. Otherwise the attempt is rejected. Every time when two monomers are connected with a bond all monomers of the new cluster take the value of the smaller cluster index. As a result, in the final structure all monomers will have the cluster index of 1. This procedure is iterated until all monomers are connected in the same cluster. The random hyperbranched polymers obtained with the QG model have, according to eqn (B1), the degree of branching DB = 0.5.[46,70]

C Hyperbranched structures obtained by the bond fluctuation method in three dimensions

To take into account excluded volume effects during the growth process we use the BFM-algorithm[52,53] for the creation and simulation of the hyperbranched structures. In this coarse-grained model, the repeat units are modeled as cubes occupying eight corners on a simple cubic lattice and the connectivity between the monomers (cubes) is given by a set of 108 bond vectors out of permutations of six basic vectors. Monte-Carlo-sampling is then generated by successive jumps of a randomly chosen monomeric unit along a randomly chosen unit vector of the lattice. The monomer can be moved to the new position if the targeted place is not occupied (excluded volume) and all existing bonds belonging to the bond vector set (cut-avoidance). The basic time unit is defined as one Monte-Carlo-step, which corresponds to one attempted monomer move in average.

For the QG model we set-up random configurations of unconnected single cubes with a volume occupation of 0.5 on the cubic lattice with size $L = 128$ ($L = 64$) and applying periodic boundary conditions in all directions. This leads to a total amount of unconnected monomers of $N_{tot} = 131,072$ (16, 384) at the beginning, where every monomer corresponds to a AB_2-functional group within the model. At the beginning of the reaction process we introduce two lists for every monomer. The first list contains the information on available functional units (AB_2, AB, A, B_2, B, or non-reactive) of the monomer and the second list represents the cluster index that the monomer belongs to. During the course of motion monomers can collide with each other face-to-face (exactly 4 corners of the moving cube collide with exactly 4 corners of another cube). If this happens a bond can be formed between them if different reactive types of monomers collide and if both monomers do not belong to the same cluster avoiding intra-molecular loops. This formation of the additional bond will alter the topology of the cluster and has to be noticed in the two lists. In the first list the information of the type of monomers will be updated. Thus, the type changes accordingly to AB, A, B_2, B, or non-reactive depending on the reaction types. In the second list the cluster index with the biggest value is replaced for all cluster monomers with the smaller index of the reactants. This modified BFM-algorithm is repeated until the size of the biggest cluster has reached the desired number of monomers N.

After the reaction process is completed the biggest cluster is placed into an empty lattice. Then, the standard BFM-algorithm is applied for Monte-Carlo-sampling for 2×10^9 MC-steps either with or without excluded volume constraints realized by switching on/off the lattice occupation check. The mean squared radius of gyration is calculated by:

$$R^2 = \frac{1}{N}\sum_{i=1}^{N}(\mathbf{r}_i - \mathbf{r}_{COM})^2, \qquad \text{(C1)}$$

where $\mathbf{r}_{COM}$ denotes the position of the center-of-mass of the hyperbranched structure and $\mathbf{r}_i$ denotes the position of the monomer i and we perform a time-average every 250 000 MC-steps. The overall procedure of creating the hyperbranched structure and evaluating the properties of the biggest cluster is repeated at least 20 times and ensemble averaged for the cluster sizes N. The initial number of unconnected monomers N_{tot} and therefore the lattice dimensions are set to $L = 64$ for $64 \leq N \leq 512$ and $L = 128$ for $512 \leq N \leq 4096$.

For the SG model with excluded volume the initial configuration is a linear chain made of 3 monomers. The lattice properties and degree of polymerization were the same as for

the QG model. The procedure for the random growth process is as follows: first we randomly choose one monomer from the existing structure. Then, we check the number of the already existing bonds of the chosen monomer. If this number is less than 3 we continue by checking if there is a vacant place on the lattice for the new monomer within the set of the smallest bond vectors. If this is the case a new monomer is added to the structure. If one of the criteria is failed a new monomer from the existing structure is randomly selected. The growth of the hyperbranched structure continues until the desired number of monomers, N, is reached. The polymer is moved according to the rules of the BFM. One attempted growth event is followed by several MC moves in order to relax the structure also during the growth. In this way, the growth proceeds in a dynamic environment respecting excluded volume constraints at any time. When the desired number of repeat units in the hyperbranched polymer is reached the simulation proceeds as for the QG model. Again we consider both, relaxation with and without excluded volume effects.

We emphasize that simulation of hyperbranched polymers even if they are relaxed without excluded volume constraints differs *a priori* from the *ad hoc* constructed structures since during the growth process excluded volume constraints are always considered. The simulation of phantom polymers are useful first to compare with the *ad hoc* constructed polymer structures and second to implement the results into the mean-field model of eqn (7).

Acknowledgements

We acknowledge financial support by the DFG with the project So 277/6-2. A. J. thanks Professor Titus Beu and Dr Michael Lang for the very fruitful discussions. J. U. S. acknowledges support by the Fonds der Chemischen Industrie (FCI).

References

1 C. Cai and Z. Y. Chen, *Macromolecules*, 1997, **30**, 5104.
2 Z. Y. Chen and C. Cai, *Macromolecules*, 1999, **32**, 5423.
3 A. A. Gurtovenko, D. A. Markelov, Y. Y. Gotlib and A. Blumen, *J. Chem. Phys.*, 2003, **119**, 7579.
4 F. Ganazzoli, R. La Ferla and G. Raffaini, *Macromolecules*, 2001, **34**, 4222.
5 P. Biswas, R. Kant and A. Blumen, *Macromol. Theory Simul.*, 2000, **9**, 56.
6 P. Biswas, R. Kant and A. Blumen, *J. Chem. Phys.*, 2001, **114**, 2430.
7 A. A. Gurtovenko, Y. Y. Gotlib and A. Blumen, *Macromolecules*, 2002, **35**, 7481.
8 J. Kemp and Z. Y. Chen, *Phys. Rev. E: Stat. Phys., Plasmas, Fluids, Relat. Interdiscip. Top.*, 1997, **56**, 7017.
9 W. Burchard, *Adv. Polym. Sci.*, 1999, **143**, 113.
10 J. J. Freire, *Adv. Polym. Sci.*, 1999, **143**, 35.
11 A. A. Gurtovenko and A. Blumen, *Adv. Polym. Sci.*, 2005, **182**, 171.
12 M. Dolgushev and A. Blumen, *Macromolecules*, 2009, **42**, 5378.
13 M. Dolgushev and A. Blumen, *J. Chem. Phys.*, 2010, **132**, 124905.
14 F. Fuerstenberg, M. Dolgushev and A. Blumen, *J. Chem. Phys.*, 2012, **136**, 154904.
15 J. Roovers, in *Star and Hyperbranched Polymers*, ed. M. K. Mishra and S. Kobayashi, Marcel Dekker, New York, 1999, p. 285.
16 C. von Ferber and A. Blumen, *J. Chem. Phys.*, 2002, **116**, 8616.
17 C. S. Jayanthi, S. Y. Wu and J. Cocks, *Phys. Rev. Lett.*, 1992, **69**, 1955.
18 C. S. Jayanthi and S. Y. Wu, *Phys. Rev. B: Condens. Matter Mater. Phys.*, 1994, **50**, 897.
19 A. Blumen, A. Jurjiu, Th. Koslowski and Ch. von Ferber, *Phys. Rev. E: Stat., Nonlinear, Soft Matter Phys.*, 2003, **67**, 061103.
20 A. Jurjiu, T. Koslowski, C. von Ferber and A. Blumen, *Chem. Phys.*, 2003, **294**, 187.
21 A. Blumen, Ch. von Ferber, A. Jurjiu and Th. Koslowski, *Macromolecules*, 2004, **37**, 638.
22 A. Blumen, A. Volta, A. Jurjiu and T. Koslowski, *Physica A*, 2005, **356**, 12.
23 A. Volta, M. Galiceanu and A. Jurjiu, *J. Phys. A: Math. Theor.*, 2010, **43**, 105205.
24 M. Dolgushev, G. Berezovska and A. Blumen, *J. Chem. Phys.*, 2010, **133**, 154905.
25 M. Dolgushev, G. Berezovska and A. Blumen, *Macromol. Theory Simul.*, 2011, **20**, 621.
26 B. Wu, Y. Lin, Z. Z. Zhang and G. R. Chen, *J. Chem. Phys.*, 2012, **137**, 044903.
27 F. Fuerstenberg, M. Dolgushev and A. Blumen, *J. Chem. Phys.*, 2013, **138**, 034904.
28 B. Wu and Z. Z. Zhang, *J. Chem. Phys.*, 2013, **139**, 024106.
29 A. Julaiti, B. Wu and Z. Z. Zhang, *J. Chem. Phys.*, 2013, **138**, 204116.
30 H. X. Liu and Z. Z. Zhang, *J.Chem. Phys.*, 2013, **138**, 114904.
31 A. Jurjiu, A. Volta and T. Beu, *Phys. Rev. E: Stat., Nonlinear, Soft Matter Phys.*, 2011, **84**, 011801.
32 M. Rubinstein and R. H. Colby, *Polymers Physics*, Oxford University Press, New York, 2003.
33 B. I. Voit, *Acta Polym.*, 1995, **46**, 87.
34 B. I. Voit and A. Lederer, *Phys. Rev. E: Stat., Nonlinear, Soft Matter Phys.*, 2011, **84**, 011801.
35 B. H. Zimm and W. H. Stockmayer, *J. Chem. Phys.*, 1949, **17**, 1301.
36 T. C. Lubensky and J. Isaacson, *Phys. Rev. A: At., Mol., Opt. Phys.*, 1979, **20**, 2130.
37 M. E. Cates, *J. Physique*, 1985, **46**, 1059.
38 D. Stauffer, A. Coniglio and M. Adam, *Adv. Polym. Sci.*, 1982, **44**, 103.
39 D. Stauffer and A. Aharony, *Introduction to percolation*, Taylor and Francis, London, 1992.
40 T. A. Vilgis, *Physica A*, 1988, **153**, 341.
41 T. A. Vilgis, *J. Physique*, 1988, **49**, 1481.
42 T. A. Vilgis, *J. Physique II*, 1992, **2**, 2097.
43 D. M. A. Buzza, *Eur. Phys. J. E: Soft Matter Biol. Phys.*, 2004, **13**, 79.
44 D. Konkolewicz, R. G. Gilbert and A. A. Gray-Weale, *Phys. Rev. Lett.*, 2007, **98**, 238301.

45 D. Konkolewicz, O. Thorn-Seshold and A. Gray-Weale, *J. Chem. Phys.*, 2008, **129**, 054901.
46 D. Hölter and H. Frey, *Acta Polym.*, 1997, **48**, 298.
47 M. Doi and S. F. Edwards, *The Theory of Polymer Dynamics*, Clarendon, Oxford, 1986.
48 J.-U. Sommer and A. Blumen, *J. Phys. A: Math. Gen.*, 1995, **28**, 6669.
49 R. Kant, P. Biswas and A. Blumen, *Macromol. Theory Simul.*, 2000, **9**, 608.
50 H. Schiessel, *Phys. Rev. E: Stat. Phys., Plasmas, Fluids, Relat. Interdiscip. Top.*, 1995, **57**, R5775.
51 J. Roovers and B. Comanita, *Adv. Polym. Sci.*, 1999, **142**, 179.
52 I. Carmesin and K. Kremer, *Macromolecules*, 1988, **21**, 2819.
53 H. P. Deutsch and K. Binder, *J. Chem. Phys.*, 1991, **94**, 2294.
54 J. S. Klos and J.-U. Sommer, *Macromolecules*, 2009, **42**, 4878.
55 W. Kuhn, *Kolloid-Z.*, 1934, **68**, 2.
56 P. J. Flory, *Principles of Polymer Chemistry*, Cornell University Press, Ithaca, 1953.
57 J. E. Martin and B. E. Eichinger, *J. Chem. Phys.*, 1978, **69**, 4588.
58 B. E. Eichinger and J. E. Martin, *J. Chem. Phys.*, 1978, **69**, 4595.
59 D. Boris and M. Rubinstein, *Macromolecules*, 1996, **29**, 7251.
60 J. S. Klos and J.-U. Sommer, *Macromolecules*, 2010, **43**, 10659.
61 B. T. Smith, J. M. Boyle, J. J. Dongarra, B. S. Garbow, Y. Ikebe, V. C. Klema, and C. B. Moler, *Matrix Eigensystem Routines - EISPACK Guide, Lecture Notes in Computer Science*, Springer, Berlin, 1976, vol. 6.
62 B. S. Garbow, J. M. Boyle, J. J. Dongarra, and C. B. Moler, *Matrix Eigensystem Routines - EISPACK Guide Extension, Lecture Notes in Computer Science*, Springer, Berlin, 1977, vol. 51.
63 J. Bunch, J. J. Dongarra, C. B. Moler and G. W. Stewart, *LINPACK User's Guide*, SIAM, Philadelphia, PA, 1979.
64 S. Alexander and R. Orbach, *J. Physique Lett.*, 1982, **69**, L625.
65 *Fractals and disordered Systems*, ed. A. Bunde and S. Havlin, Springer, Berlin, 1991.
66 M. G. Cosenza and R. Kapral, *Phys. Rev. A: At., Mol., Opt. Phys.*, 1992, **46**, 1850.
67 M. E. Cates, *Phys. Rev. Lett.*, 1984, **53**, 926.
68 R. L. Ferla, *J. Chem. Phys.*, 1997, **106**, 688.
69 S. Rathgeber, M. Monkenbusch, J. L. Hedrick, M. Trollsas and A. P. Gast, *J. Chem. Phys.*, 2006, **125**, 204908.
70 D. Hölter, A. Burgath and H. Frey, *Acta Polym.*, 1997, **48**, 30.